Scientific paper

1*H*-Indole-2,3-dione 3-thiosemicarbazones Carrying a 4-sulfamoylphenyl Moiety with Selective Antiviral Activity Against Reovirus-1

Füsun Göktaş,[1] Gizem Nur Duran,[2] Mehmet Özbil,[3] Özge Soylu-Eter[1,*] and Nilgün Karalı[1]

[1] *Department of Pharmaceutical Chemistry, Faculty of Pharmacy, Istanbul University, Istanbul, Turkey*

[2] *Department of Chemistry, Institute of Science and Technology, Marmara University, Istanbul, Turkey*

[3] *Department of Biotechnology, Institute of Biotechnology, Gebze Technical University, Kocaeli, Turkey*

** Corresponding author: E-mail: ozge.soylu@istanbul.edu.tr*
Tel.: +902124400000 (Internal 13462)

Received: 12-18-2023

Abstract

1*H*-Indole-2,3-dione 3-[4-(4-sulfamoylphenyl)thiosemicarbazones] **6a**–**j** were evaluated against para-influenza-3, reovirus-1, sindbis, coxsackie B4, and Punto Toro viruses. New 1-methyl-1*H*-indole-2,3-dione 3-[4-(4-sulfamoylphenyl) thiosemicarbazones] **7a**–**c** were synthesized to evaluate the contribution of methyl substitution at position 1 of the indole ring to antiviral activity. The test results showed that 5-trifluoromethoxy substituted compound **6c** (EC_{50} 2–9 μM) and 5-bromo substituted **6f** (EC_{50} 2–3 μM) have non-toxic selective antiviral activity, while not all standards are active against reovirus-1. Molecular docking studies of **6c** and **6f** were carried out to determine the possible binding positions with reovirus-1. Trifluoromethoxy and bromine substitutions at position 5 of the indole ring provided selective antiviral activity, while methyl substitution at position 1 of the indole ring significantly decreased the activity against reovirus-1 and increased toxicity.

Keywords: 1*H*-indole-2,3-dione; thiosemicarbazone; molecular modeling; antiviral activity; reovirus-1.

1. Introduction

Viral pathogenesis examines how a virus interacts with the host at multiple levels when a virus infects a host. Although the pathogenesis of each virus is different, there are many common points shared among all pathogenic viruses in the virus life cycle. When understanding the mechanism according to which the disease develops provides a significant benefit in the development of effective therapies. Virus mediated disease processes can be developed by taking into consideration the common aspects of some general concepts in viral pathogenesis.[1,2]

Reoviruses are useful models to understand the relationship between viral entry and patogenesis.[3,4] Reoviruses are non-enveloped, double-stranded RNA viruses in the family *Reoviridae*. Most mammalian species, including humans, serve as hosts for reovirus infection. Reoviruses attach to host cells via the filamentous attachment protein σ1. The σ1 protein of all reovirus serotypes engages junctional adhesion molecule-A (JAM-A). Reoviruses have 3 major serotypes: reovirus type 1 (strain Lang) (T1L) (mammalian orthovirus 1), type 2 Jones (T2J) and type 3 Dearing (T3D), which differ primarily in σ1 sequence.[5–8] The three serotypes share a common complement fixation antigen but can be distinguished by hemagglutination inhibition and neutralization techniques.[4] The gastrointestinal (GI) tract is a portal of entry for reoviruses. Reovirus serotype 1 strain Lang was shown to specifically infect the epithelial cells of the ileum and disrupt the intestinal immune homeostasis, while sparing the epithelial cells in the duodenum, jejunum, and colon.[9,10] Advanced reovirus studies have provided much information about the mechanisms underlying viral replication and pathogenesis.[11,12] However, *Reoviridae* viruses have limited ability to make specific changes to the genome. Today, a specific treatment or protection measures cannot be recommended because of the lack of a definite relationship in the disease for people with reovirus infections.

1*H*-Indole-2,3-dione (isatin) is a heterocyclic compound which has been known for nearly 150 years and is involved in many pharmacological activities. Isatin is also a highly versatile substrate that can be used in the preparation of a wide variety of heterocyclic compounds for drug synthesis and is a versatile precursor for many biologically active molecules. There are many studies on isatin 3-thiosemicarbazone derivatives with antiviral activity, too.[13–17] Methisazone (1-methylisatin 3-thiosemicarbazone) (**I**) is the first compound approved by Food and Drug Administration (FDA) for treatment of the vaccinia virus causing smallpox.[18,19] It has been determined that 1-methylisatin 3-(4,4'-diethylthiosemicarbazone) (**II**) inhibits the moleney murine leukemia virus.[20] **II** and 1-allylisatin 3-(4,4'-diallylthiosemicarbazone) (**III**) show significantly selective anti-HIV activity.[21] Antiviral activities of isatin 3-thiosemicarbazone derivatives against HSV-1 and HSV-2 viruses were investigated, and SAR studies revealed that the thiourea group in the thiosemicarbazone structure and the nitrogen of the isatin ring play an important role in antiviral activity. As a result of the research, it was determined that derivatives carring various substituents as methyl, ethyl, phenyl and benzyl at position 1 of isatin do not show antiviral activity, and the most effective derivative (IC_{50} 1.54 ± 0.21 μM) against HSV-2 virus was the compound **IV** carrying a diethyl group at the thiosemicarbazone residue. The compound **V** carrying a morpholinyl ring at the thiosemicarbazone residue showed the highest inhibition (IC_{50} 1.30 ± 0.16 and 2.74 ± 0.23 μM) against HSV-1 and HSV-2 viruses, respectively. Moreover, the compound **VI** (IC_{50} 2.20 ± 0.34–5.90 ± 0.26 μM) bearing a 5-methoxy or trifluoromethoxy group as R_1 and a hydrogen, 3-methyl, 3-methoxy, 4-methoxy, 4-chlorine or 4-bromine group as R_2 were found to be selectively effective against HIV-1 virus.[22] The antiviral activities of a series of isatin 3-thiosemicarbazones were examined against vaccinia and cowpox viruses, and their effects were compared with metisazone and cidofovir. Among the tested compounds, the compound **VII** was found to be the strongest inhibitor against vaccinia (EC_{50} 0.6 ± 6.8 μM) and cowpox (EC_{50} 6.0 ± 2.9 μM) viruses and its antiviral activity was stronger than metisazone and cidofovir. Moreover, 5-bromoisatin has been defined as the key pharmacophore for better antiviral activity (Figure 1).[23]

Many studies have been carried out to evaluate the broad-spectrum antiviral activities of 3-imino isatin derivatives carrying the 4-sulfamoylphenyl residue. The inhibitory activities of 4-[(1,2-dihydro-2-oxo-3*H*-indol-3-ylidene) amino]-*N*-(4,6-dimethyl-2-pyrimidinyl)-benzenesulfonamide (**VIII**) and its derivatives against vaccinia and cowpox viruses that cause smallpox were tested *in vitro*. While 5-methylisatin derivative (EC_{50} 18 μM) showed the strongest activity against vaccinia virus, 1-acetylisatin derivative showed strong inhibitory effect against cowpox virus.[24] **VIII** and its derivatives were tested against influenza A and B viruses. Among the compounds tested, **VIII** and its 5-chloro, 5-bromo, 5-methyl and *N*-acetyl derivatives were found to be effective against the H1N1 (EC_{50} 13.8–26.0 μg/mL), H3N2 (EC_{50} 2.7–5.2 μg/mL) and H5N1 (EC_{50} 3.1–6.3 μg/mL) strains of influenza A, and influenza B (EC_{50} 7.7–11.5 μg/mL).[25] **VIII** and its derivatives were also tested against the 2009 pandemic influenza (H1N1) virus and all compounds were found to inhibit the replication of the virus and the most active compound was the 5-bromoisatin derivative (EC_{50} 27 μM).[26] In the study in which some derivatives of **VIII** were tested against HCV and SARS-CoV viruses, it was determined that the 5-fluoroisatin derivative inhibited the HCV RNA synthesis at 6 μg/mL and provided 45% protection against SARS-CoV replication. The results obtained

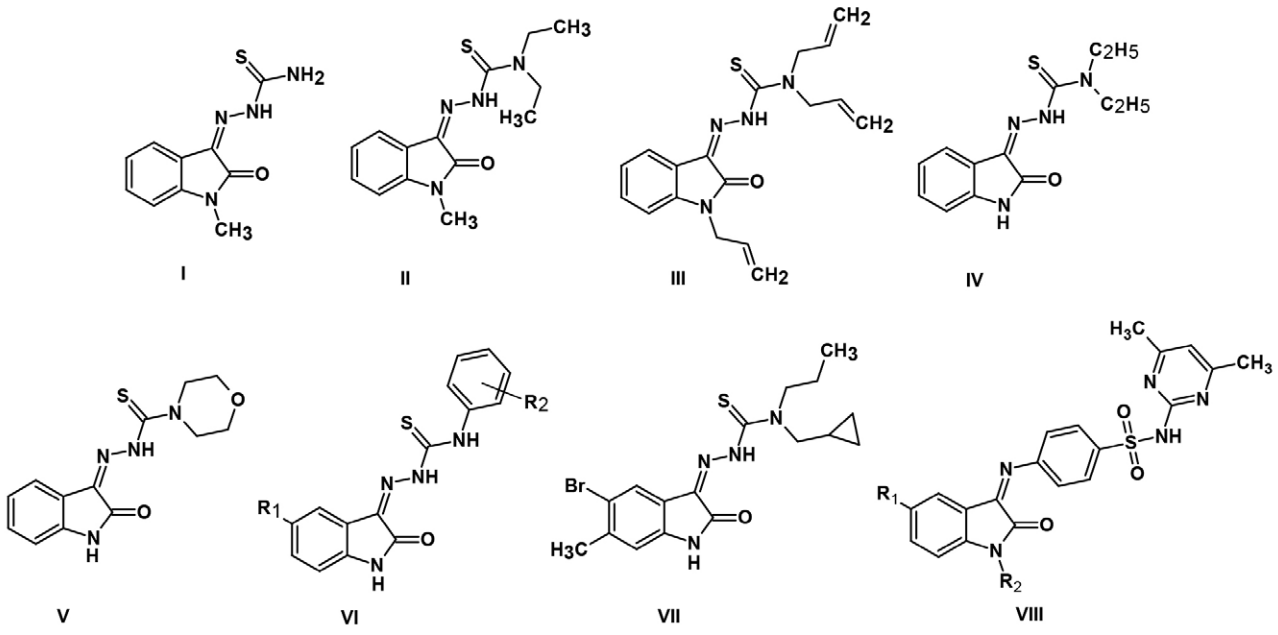

Figure 1. Structures of 2-indolinone derivatives **I**–**VIII** with antiviral activity

showed that sulfonamide side chain was important in **VIII** and its derivatives (Figure 1).[27]

In the present study, 1*H*-indole-2,3-dione 3-thiosemicarbazones **6a–j** carrying a 4-sulfamoylphenyl moiety were evaluated for *in vitro* antiviral activity against para-influenza-3 virus, reovirus-1, sindbis virus, coxsackie virus B4, and Punto Toro virus. To investigate the contribution of methyl substitution at position 1 of the indole ring to antiviral activity, new 5-substituted 1-methyl-1*H*-indole-2,3-dione 3-[4-(4-sulfamoylphenyl)thiosemicarbazones] **7a–c** were synthesized and tested.

2. Results and Discussion

2. 1. Chemistry

5-Substituted 1*H*-indole-2,3-diones **1** were reacted with methyl iodide to yield 1-methyl-5-substituted 1*H*-indole-2,3-diones **2**. (4-Sulfamoylphenyl)isothiocyanate (**4**) was obtained from the treatment of 4-aminobenzenesulfonamide (**3**) with thiophosgene. 4-(4-Sulfamoylphenyl) thiosemicarbazide (**5**) was synthesized by the reaction of **4** and hydrazine hydrate. New 5-substituted 1-methyl-1*H*-indole-2,3-dione 3-[4-(4-sulfamoylphenyl)thiosemicarbazones] **7a–c** were prepared by the condensation of **5** and **2**. The compounds **6a–j** have been previously described in the literature.[28] Analytical and spectral findings proving the analytical purity of the compounds **6a–j** are given in the Supplementary Material. The structures of new compounds **7a–c** were confirmed by elemental analysis and spectral data (IR, ^{1}H NMR, ^{13}C NMR-APT and LCMS-ESI) (Scheme 1, Experimental Section, and Supplementary Material).

IR spectra of **7a–c** showed absorption bands in the 3142–3358 cm^{-1} region for NH stretchings of the thioamide and sulfonamide functions. The bands resulting from

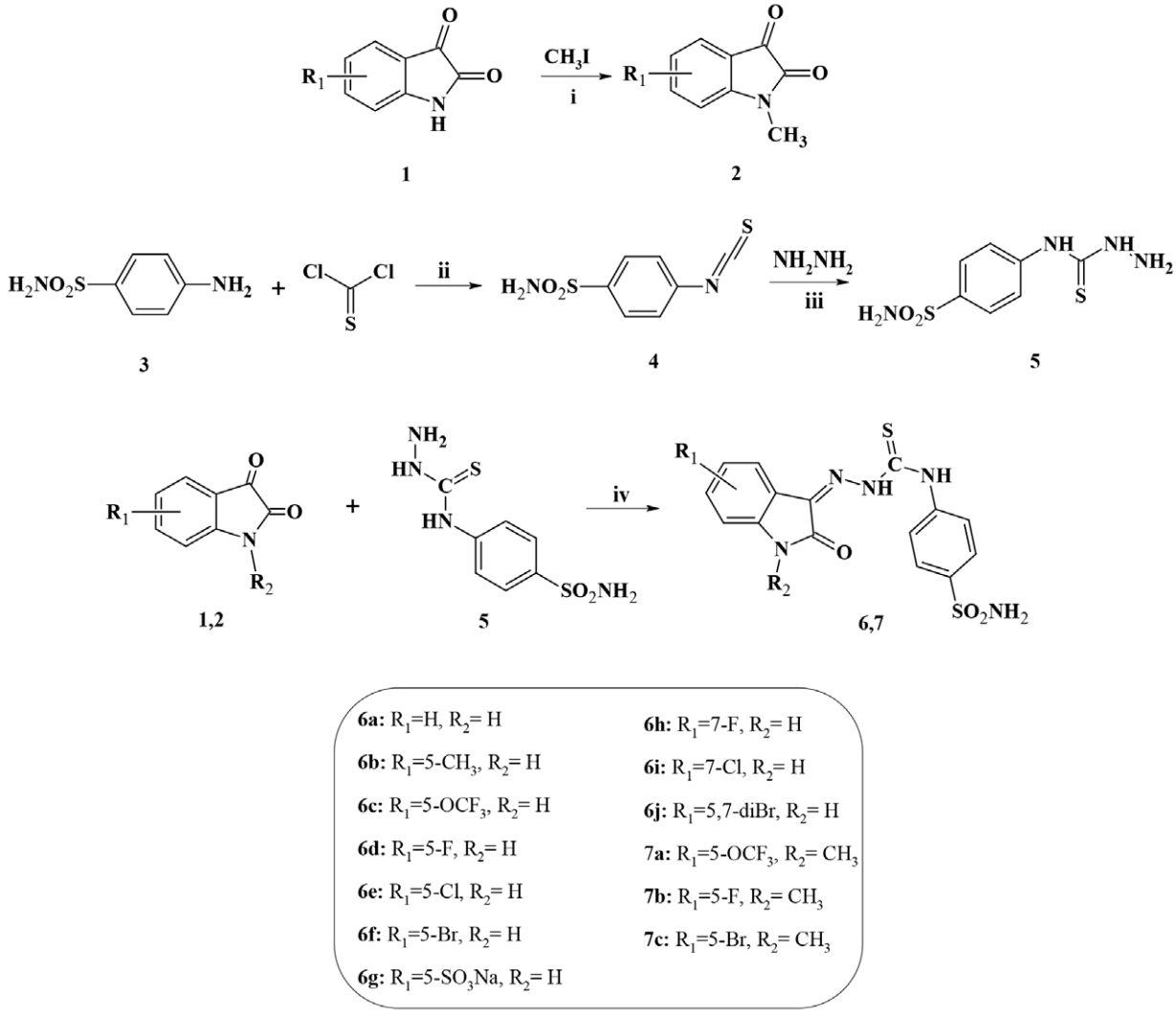

Scheme 1. Synthesis of 1*H*-indole-2,3-dione 3-[(4-sulfamoylphenyl)thiosemicarbazones] **6a–j** and **7a–c**. Reagents and conditions: *i*) DMF, K_2CO_3, KI, stirred, *ii*) H_2O, HCl, stirred, *iii*) EtOH, stirred, cooled, *iv*) EtOH, H_2SO_4, reflux.

lactam C=O and thioamide C=S stretchings appeared at 1680–1691 and 1253–1367 cm^{-1} regions, respectively. S=O stretchings of sulfonamide groups appeared at 1313–1336 and 1151–1166 cm^{-1} regions. ^{1}H NMR spectra of **7a–c** displayed singlets at δ 7.37–7.40, 11.01–11.05 and 12.65–12.71 ppm regions for sulfonamide, thiosemicarbazone N_4 and N_2 protons, respectively. The phenyl protons of 4-sulfamoylphenylthiosemicarbazone moiety which are deshielded by the electron-attracting action of the sulfonamide and thioamide groups, showed as a singlet in the δ 7.37–7.40 ppm area. The N-CH_3 and indole proton resonances of **7a–c** were assigned to the 1-methyl-2-indolinone structure. The indole C_4 and C_6 protons were deshielded by the anisotropic effect of the azomethine group at position 3 of the 2-indolinone ring. The indole C_7 proton was shielded by the mesomeric effect of the anilid NH group in the 2-indolinone ring. The indole C_4, C_6 and C_7 protons of **7a–c** showed at δ 7.67–8.04, 7.33–7.65 and 7.15–7.26 ppm regions, respectively. ^{13}C NMR-APT spectra of **7a–c** displayed signals at δ 176.75–176.86, 160.94–161.41 and 131.00–131.70 ppm regions due to C=S, indole C_2 and C_3 signals, respectively. The phenyl carbon signals were observed in the order of C_3, C_1, C_5, C_6, C_4, and C_2 starting from downfield. Indole C_2 and C_{7a} carbons showed the most downfield shift among the indole carbon signals. The indole C_7 and C_{3a} carbons in the *ortho* position of the lactam group were found to be the most shielded among the indole carbons. In the spectra, shifts were observed in the indole signals based on the nature of the substituents at position 5 of the 2-indolinone ring. The indole C_{3a}, C_4, C_5, C_6 signals in the spectra of the 5-fluorine substituted **7b**, which

Table 1. The MCC and EC_{50} values of the compounds **6** and **7** against different viruses in Vero cells.

Compound	R_1	R_2	MCC (μM)[a]	EC_{50} (μM)[b] Para-influenza-3 virus	Reovirus-1	Sindbis virus	Coxsackie virus B4	Punto Toro virus	
6a	H	H	100	>20	>20	>20	>20	>20	
6b	5-CH_3	H	100	>20	>20	>20	>20	>20	
6c	5-OCF_3	H	>100	>100	**2**	>100	>100	>100	(test1)
			100	>20	**3**	>20	>20	>20	(test2)
			>100	Not tested	**9**	Not tested	Not tested	Not tested	(test3)
6d	5-F	H	>20	>20	>20	>20	>20	>20	
6e	5-Cl	H	100	>20	>20	>20	>20	>20	
6f	5-Br	H	>20	>20	**2**	>20	>20	>20	(test1)
			100	>20	**3**	>20	>20	>20	(test2)
			100	Not tested	**2**	Not tested	Not tested	Not tested	(test3)
6g	5-SO_3Na	H	>100	>100	>100	>100	>100	>100	
6h	7-F	H	100	>100	>100	>100	>100	>100	
6i	7-Cl	H	100	>100	>100	>100	>100	>100	
6j	5,7-diBr	H	100	>20	>20	>20	>20	>20	
7a	5-OCF_3	CH_3	>20	>20	>20	>20	>20	>20	
7b	5-F	CH_3	100	>20	>20	>20	>20	>20	
7c	5-Br	CH_3	20	>4	>4	>4	>4	>4	
	DS-5000*		>100	>100	>100	4	9	9	(test1)
			>100	>100	>100	4	45	20	(test2
			>100	>100	>100	4	20	20	(test3)
	(S)-DHPA		>250	>250	>250	>250	>250	>250	(test1)
			>250	>250	>250	>250	>250	>250	(test2)
			>250	>250	>250	>250	>250	>250	(test3)
	Ribavirin		>250	126	250	>250	>250	112	(test1)
			>250	250	>250	>250	>250	>250	(test2)
			>250	250	>250	>250	>250	>250	(test3)

[a] Minimum cytotoxic concentration: required to cause a microscopically detectable alteration of normal cell morphology.
[b] Required to reduce virus-induced cytopathogenicity by 50%. * Concentration unit is μg/mL.
Note that the SI cannot be exactly calculated when the MCC is higher than the highest concentration tested.

showed that the ^{13}C–^{19}F connections were observed as separate doublets. Electrospray ionization (ESI) mass spectra of **7a**–**c** were obtained using the positive ionization technique.

2. 2. Antiviral Activity

1*H*-Indole-2,3-dione 3-[4-(4-sulfamoylphenyl)thiosemicarbazones] **6a**–**j** were evaluated against para-influenza-3 virus, reovirus-1, sindbis virus, coxsackie virus B4, and Punto Toro virus. DS-5000, (*S*)-DHPA and ribavirin were used as standards in the tests (Table 1). Among the compounds tested, the trifluoromethoxy substituted **6c**, and bromine substituted **6f** at position 5 of the indole ring showed selective antiviral activity against reovirus-1. Three independent assays were performed to derive mean fifty percent effective concentration (EC_{50}) values for **6c** and **6f**. The EC_{50} values of **6c** were determined to be 2, 3 and 9 μM and the EC_{50} values of **6f** were determined to be 2, 3 and 2 μM**.** The minimum cytotoxic concentration (MCC) values of **6c** and **6f** were determined as >100 or 100 μM, and 100 or >20 μM in Vero cells, respectively. In Table 1, data indicating antiviral activity are marked in yellow as the selectivity indexs (SI) (ratio of MCC to EC_{50}) are higher than five. The SI values of **6c** and **6f** are in the range of 10–50 in Vero cells. However, in the presence of hydrogen, methyl, chlorine or fluorine substituents at position 5 of the indole ring, the activity against reovirus-1 decreased to >20 μM. In the 5,7-dibromo substitution, the activity decreased to >20 μM, while the 5-sulfonic acid sodium or 7-fluorine and 7-chlorine substituted compounds were found to be inactive. Moreover, none of the compounds used as standard were found to be effective against reovirus-1. The EC_{50} values of DS-5000, (*S*)-DHPA and ribavirin are >100, >250, and 250 or >250 μM, respectively**.**

To investigate the contribution of methyl substitution at position 1 of the indole ring to antiviral activity, the trifluoromethoxy substituted **7a**, the fluorine substituted **7b** and the bromine substituted **7c** at position 5 of the indole ring were also evaluated against para-influenza-3 virus, reovirus-1, sindbis virus, coxsackie virus B4, and Punto Toro virus in Vero cells. The EC_{50} values of **7a**–**c** against all viruses tested were determined to be >20, >20 and >4 μM, respectively. As seen in the Table 1, the MCC values of **7a**–**c** are >20, 100 and 20 μM in Vero cells, respectively. In compounds **7a** and **7c**, the introduction of a methyl group at position 1 of indole ring increased the cytotoxicity while decreasing the antiviral activity against reovirus-1.

The antiviral activities of **6c** and **6f**, which are selective and non-toxic against reovirus-1 in Vero cells, have also been investigated in HeLa cells against reovirus-1. Two independent assays were performed to derive mean fifty percent effective concentration (EC_{50}) values for **6c** and **6f**. The EC_{50} values of **6c** were determined to be 45 and 20 M and the EC_{50} values of **6f** were determined to be 45 and 45 M. The MCC values were determined to be >100 M for both **6c** and **6f** in HeLa cells. The SI value of **6c** was calculated as 5, but the SI value of **6f** was determined to be less than 5 (Table 2).

The results obtained show the importance of trifluoromethoxy and bromine substituents at position 5 of the indole ring, as well as the presence of hydrogen at position 1 of the indole ring for the selective and nontoxic effect against reovirus-1. Whereas, with 5-hydrogen, methyl, fluorine, chlorine, sulfonic acid sodium, 5,7-dibromo, 7-fluorine and 7-chlorine substitution at the indole ring, as well as 1-methyl substitution, the activity decreased or inactive derivatives were obtained. The introduction of a methyl group at position 1 of indole ring increased the cytotoxicity while decreasing the antiviral activity against reovirus-1.

Table 2. The MCC and EC_{50} values of the compounds **6c** and **6f** against reovirus-1 in HeLa cells.

Comp.	R_1	R_2	MCC (M)[a]	EC_{50} (M)[b] Reovirus-1	
6c	5-OCF_3	H	>100	**45**	(test1)
			>100	**20**	(test2)
6f	5-Br	H	>100	**45**	(test1)
			>100	**45**	(test 2)
DS-5000*			>100	>100	(test1)
			>100	>100	(test2)
(S)-DHPA			>250	>250	(test1)
			>250	>250	(test2)
Ribarivin			>250	112	(test1)
			>250	>250	(test2)

[a] Minimum cytotoxic concentration: required to cause a microscopically detectable alteration of normal cell morphology. [b] Required to reduce virus-induced cytopathogenicity by 50%. * Concentration unit is g/mL.
Note that the SI can not be exactly calculated when the MCC is higher than the highest concentration tested.

Table 3. List of amino acids and interactions forming binding site of the compounds **6c** and **6f** and binding energies.

Ligand	Binding site residues	Interaction type	Interacting atoms (protein-ligand)	Binding free energy (kcal/mol)
6c	Arg312	H-Bonding	NH1–F1	**–24.1**
	Arg312	H-Bonding	NH2–F2	
	Arg312	H-Bonding	NH2–O3	
	Tyr313	T-shaped π-π Stacking	Phenyl ring–Phenyl ring	
	Val326	Hydrophobic	Side chain carbons–Indole ring	
	Arg329	H-Bonding	NEH–O2	
	Phe330	Hydrophobic	Phenyl ring–Indole ring	
	Gly331	Hydrophobic	Side chain carbons–Phenyl ring	
	Met332	H-Bonding	NH–O2	
	Met332	H-Bonding	O–NH4	
	Lys360	Hydrophobic	Side chain carbons–Aliphatic chain	
	Asp362	Hydrophobic	Side chain carbons–Indole ring	
	Asp363	H-Bonding	OD2–NH	
6f	Trp350	π-π Stacking	Indole ring–Indole ring	**–14.4**
	Arg351	Hydrophobic	Side chain carbons–Indole ring	
	Ala352	Hydrophobic	CB–Aliphatic chain	
	Val354	Hydrophobic	Side chain carbons–Phenyl ring	
	Ser370	H-Bonding	OGH–O2	
	Gln371	Hydrophobic	Side chain carbons	
	Met372	Hydrophobic	Side chain carbons–Phenyl rings	
	Thr373	H-Bonding	NH–N_4	
	Thr374	Hydrophobic	Side chain carbons	
	Asn375	Hydrophobic	Side chain carbons–Phenyl ring	
	Ser376	Hydrophobic	Side chain carbons–Indole ring	

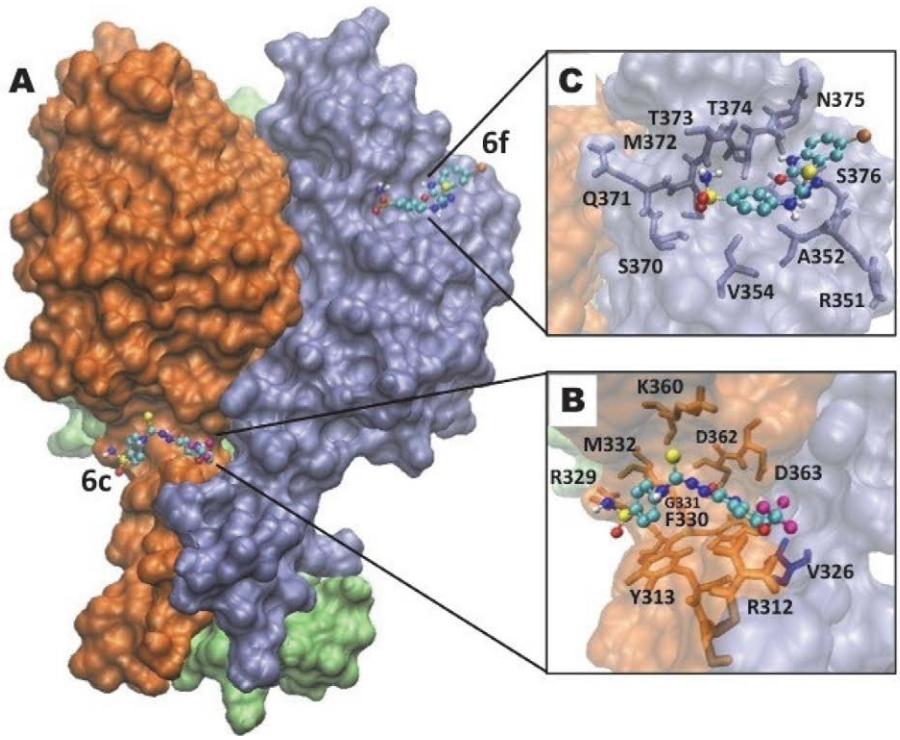

Figure 2. (**A**) The binding sites for **6c** and **6f** are shown (three monomers of T1L are in different colors), (**B**) Detailed view of binding site for **6c**, interacting residues are labelled. (**C**) Detailed view of binding site for **6f**, interacting residues are labelled.

2. 3. Molecular Modeling

The lowest energy structures obtained from molecular dynamics (MD) simulations revealed the most probable binding sites for the compounds **6c** and **6f** (Figure 2A). Moreover, binding free energies from MD simulations revealed that **6c** binds with 9.7 kcal/mol lower free energy than **6f**.

Compound **6c** was buried in between two homodimers in the homotrimer structure of T1L protein (Figure 2A). The binding pocket for **6c** was formed by amino acid residues Arg312, Tyr313, Val326, Arg329, Phe330, Gly331, Met332, Lys360, Asp362 and Asp363 (Figure 2B). It bound to the protein mostly through hydrogen (H-) bondings in addition to few hydrophobic interactions (Table 3). Hydrophobic interactions were mainly governed by its indole ring. Reason for this placement was -OCF_3 group, which interacts with the residue Arg312 of one monomer, which in return interacted with Gln325 residue of the second monomer at the body part of T1L protein. This must be the reason for lower binding energy for compound **6c**.

The binding site of compound **6f** was located in the head domain of one of the monomers in the homotrimer structure of T1L protein (Figure 2A). It bound to the site formed by amino acid residues Trp350, Arg351, Ala352, Val354, Ser370, Gln371, Met372, Thr373, Thr374, Asn375 and Ser376 (Figure 2C). Interactions were mainly hydrophobic, mostly governed by indole and phenyl rings of the ligand (Table 3). The trifluoromethoxy group in **6c**, was replaced by bromine in **6f**, which affects the binding site and nature of the interactions. This binding pocket was very similar to the GM2 glycan binding site.[29] The potent inhibitory activity of this molecule observed in this present study might be due to this critical binding site.

3. Materials and Methods

3. 1. Chemistry

3. 1. 1. General

Melting points of the synthesized derivatives were recorded in open capillaries using a Büchi B-540 Melting Point apparatus and are uncorrected. IR spectra (as KBr discs) were measured with a Shimadzu IR Affinity-1 FTIR spectrophotometer. ^{1}H and ^{13}C NMR spectra were obtained on Varian UNITY INOVA 500 MHz and Bruker Avance NEO 500 MHz spectrophotometers in DMSO-d_6. Mass spectra were recorded on a Thermo Finnigan LCQ Advantage Max spectrometer. Analytical data were obtained on Thermo Finnigan Flash EA 1112 elemental analyzer.

3. 1. 2. Synthesis of 1-methyl-5-substituted 1*H*-indole-2,3-diones 2[30–32]

1*H*-Indole-2,3-diones **1** (5 mmol) and 0.97 g of anhydrous potassium carbonate (K_2CO_3, MW: 138.21, 7 mmol) are stirred in 10 mL of *N*,*N*-dimethylformamide (DMF, MW: 73.09) at room temperature for 1 h. After the addition of methyl iodide (CH_3I, MW: 141.94, 15 mmol) and 0.17 g of anhydrous potassium iodide (KI, MW: 166.00, 1 mmol) as a catalyst, the reaction is heated to 50–60 °C until completed. The reaction mixture was evaporated to dryness under reduced pressure, washed with ice water and recrystallized from ethanol.

3. 1. 3. Synthesis of 4-(isothiocyanato) benzenesulfonamide (4)[33]

4-Aminobenzenesulfonamide (**3**) (MW: 172.20, 3 mmol) was dissolved in 50 mL of water containing 12 mL of concentrated hydrochloric acid (HCl, MW: 36.46). To the solution, thiophosgene ($CSCl_2$, MW: 114.98, 3 mmol) was added in one portion. Stirring was begun immediately and continued until all of the red color of $CSCl_2$ disappeared and the product appeared as a white crystalline precipitate. The precipitate was filtered and washed thoroughly with water.

3. 1. 4. Synthesis of 4-(4-sulfamoylphenyl) thiosemicarbazide (5)[28]

To a solution of hydrazine hydrate ($NH_2NH_2{\cdot}H_2O$, MW: 50.06, 5 mmol) in 10 mL of ethanol, a suspension of 1.07 g of 4-(isothiocyanato)benzenesulfonamide (**4**) (MW: 214.26, 5 mmol) in ethanol (10 mL) was added dropwise with stirring and cooling in an ice bath. The mixture was allowed to stand overnight. The crystals formed were recrystallized from ethanol.

3. 1. 5. Synthesis of 5-(non)substituted 1*H*-indole-2,3-dione 3-[4-(4-sulfamoylphenyl) thiosemicarbazones] 6a–j[28,34,35]

0.86 g of 4-(4-sulfamoylphenyl)thiosemicarbazide (**5**) (MW: 246.3099, 3.5 mmol) was added to the solution of 1*H*-indole-2,3-diones **1a–j** (3.5 mmol) in ethanol (20 mL) containing a catalytic amount of concentrated sulfuric acid (H_2SO_4, MW: 98.08). The mixture was refluxed on a water bath. The product formed after cooling was filtered and washed with ethanol or recrystallized from ethanol. The compounds **6a–j** have been previously described by Karalı *et al.*[33] Experimental information for these molecules is given in the Supplementary Material.

3. 1. 6. Synthesis of 1-methyl-5-substituted 1*H*-indole-2,3-dione 3-[4-(4-sulfamoylphenyl) thiosemicarbazones] 7a–c[28,34,35]

0.86 g of 4-(4-sulfamoylphenyl)thiosemicarbazide (**5**) (MW: 246.3099, 3.5 mmol) was added to the solution of 5-substituted 1-methyl-1*H*-indole-2,3-diones **2** (3.5

mmol) in ethanol (20 mL) containing a catalytic amount of concentrated sulfuric acid (H_2SO_4, MW: 98.08). The mixture was refluxed on a water bath. The product formed after cooling was filtered and washed with ethanol or recrystallized from ethanol.

1-Methyl-5-(trifluoromethoxy)-1*H*-indole-2,3-dione 3-[4-(4-Sulfamoylphenyl)-thiosemicarbazone] (7a). Orange powder (1.16 g, 70%), mp 241–243 °C; IR (KBr): 3358, 3269 (NH), 1681 (C=O), 1616, 1573, 1519, 1479 (C=N, C=C), 1336, 1151 (S=O), 1211 (C=S), 1151 (C-F). ^{1}H NMR (DMSO-d_6, 500 MHz) δ 3.25 (s, 3H, NCH_3), 7.26 (1H, dd, J = 7.8, 1.0 Hz, ind. C_7-H), 7.37 (2H, s, SO_2NH_2), 7.48 (1H, d, J = 7.8 Hz, ind. C_6-H), 7.78 (1H, s, ind. C_4-H), 7.86 (4H, s, phen.), 11.03 (1H, s, N_4-H), 12.69 (1H, s, N_2-H). ^{13}C NMR (^{13}C NMR-APT, DMSO-d_6, 125 MHz) **δ** 26.44 (ind. N-CH_3), 111.63 (ind. C_7), 114.77 (ind. C_4), 120.68 (q, J = 256.1 Hz, OCF_3), 121.08 (ind. C_{3a}), 124.74 (ind. C_6), 126.04 (phen. $C_{2,6}$), 126.54 (phen. $C_{3,5}$), 131.34 (ind. C_3), 141.67 (phen. C_4), 141.85 (phen. C_1), 143.17 (ind. C_{7a}), 144.48 (ind. C_5), 161.41 (ind. C_2), 176.86 (CS). LCMS (ESI (+)) $C_{17}H_{15}F_3N_5O_4S_2$ [M+H]$^+$: 474.456761; found [M+H]$^+$: 474.00. Anal. Calcd for $C_{17}H_{14}F_3N_5O_4S_2.{}^1/_2H_2O$ (482.4570096): C, 42.32; H, 3.13; N, 14.51; found: C, 42.41; H, 2.80; N, 14.85.

1-Methyl-5-fluoro-1*H*-indole-2,3-dione 3-[4-(4-Sulfamoylphenyl)thiosemicarbazone] (7b). Orange powder (1.21 g, 85%), mp 265–268 °C; IR (KBr): 3305, 3228, 3116 (NH), 1680 (C=O), 1618, 1597, 1541, 1475 (C=N, C=C), 1332, 1161 (S=O), 1217 (C=S), 1151 (C-F). ^{1}H NMR (DMSO-d_6, 500 MHz) δ 3.22 (s, 3H, NCH_3), 7.19 (1H, dd, J = 8.4, 4.0 Hz, ind. C_7-H), 7.33 (1H, dt, J = 8.4, 2.8 Hz, ind. C_6-H), 7.39 (2H, s, SO_2NH_2), 7.67 (1H, dd, J = 8.0, 2.4 Hz, ind. C_4-H), 7.87 (4H, s, phen.), 11.01 (1H, s, N_4-H), 12.71 (1H, s, N_2-H). ^{13}C NMR (^{13}C NMR-APT, DMSO-d_6, 125 MHz) **δ** 26.38 (ind. N-CH_3), 108.71 (d, J = 26.1 Hz, ind. C_4), 111.58 (d, J = 7.8 Hz, ind. C_7), 118.03 (d, J = 24.2 Hz, ind. C_6), 121.00 (d, J = 9.3 Hz, ind. C_{3a}), 125.83 (phen. $C_{2,6}$), 126.52 (phen. $C_{3,5}$), 131.70 (ind. C_3), 140.57 (ind. C_{7a}), 141.69 (phen. C_4), 141.73 (phen. C_1), 159.16 (d, J = 238.3 Hz, ind. C_5), 161.29 (ind. C_2), 176.75 (CS). LCMS (ESI (+)) $C_{16}H_{15}FN_5O_3S_2$ [M+H]$^+$: 408.4498546; found [M+H]$^+$: 408.00. Anal. Calcd for $C_{16}H_{14}FN_5O_3S_2.{}^1/_2H_2O$ (416.4501032): C, 46.14; H, 3.63; N, 16.81; found: C, 45.94; H, 3.07; N, 17.25.

1-Methyl-5-bromo-1*H*-indole-2,3-dione 3-[4-(4-Sulfamoylphenyl)thiosemicarbazone] (7c). Orange powder (1.42 g, 87%), mp 275–277 **°C; IR (KBr): 3305, 3236, 3142 (NH), 1680 (C=O), 1595, 1539, 1469 (C=N, C=C),** 1328, 1161 (S=O), 1217 (C=S), 831 (C-Br). ^{1}H NMR (DMSO-d_6, 500 MHz) **δ** 3.21 (s, 3H, NCH_3), 7.15 (1H, d, J = 8.4 Hz, ind. C_7-H), 7.65 (1H, dd, J = 8.4, 2.0 Hz, ind. C_6-H), 7.40 (2H, s, SO_2NH_2), 8.04 (1H, d, J = 2.0 Hz, ind. C_4-H), 7.87 (4H, s, phen.), 11.05 (1H, s, N_4-H), 12.65 (1H, s, N_2-H). ^{13}C NMR (^{13}C NMR-APT, DMSO-d_6, 125 MHz) **δ** 26.38 (ind. N-CH_3), 112.39 (ind. C_7), 115.33 (ind. C_5), 121.73 (ind. C_{3a}), 123.93 (ind. C_4), 125.95 (phen. $C_{2,6}$), 126.51 (phen. $C_{3,5}$), 131.00 (ind. C_3), 133.90 (ind. C_6), 141.68 (phen. C_4), 141.76 (phen. C_1), 143.33 (ind. C_{7a}), 160.94 (ind. C_2), 176.76 (CS). LCMS (ESI-): m/z (%) 466, 468 ([M-H]$^-$, 12, 11), 252, 254 (12, 14), 213 (100), 187 (12), 149 (18), 115, 117 (14, 16). LCMS (ESI (+)) $C_{16}H_{15}BrN_5O_3S_2$ [M+H]$^+$: 469.3554514; found [M+H]$^+$: 469.90. Anal. Calcd for $C_{16}H_{14}BrN_5O_3S_2$ (468.34806): C, 41.03; H, 3.01; N, 14.95; found: C, 40.79; H, 2.60; N, 14.74.

3. . Antiviral Activity

The compounds **6a–j** and **7a–c** were evaluated for antiviral activity against para-influenza-3, reovirus-1, sindbis virus, coxsackie virus B4, and Punto Toro virus in Vero cells and reovirus-1 in HeLa cells.[36,37] The assays were performed in 96-well plates containing semicon-fluent cell cultures. At the same time with the virus, serial dilutions of the test or reference compounds (DS-5000, (*S*)-DHPA and ribavirin) were added. After the plates were incubated at 37 °C for 3–6 days, the antiviral activities of the compounds [expressed as 50% effective concentration (EC50)] and cytotoxicity [expressed as minimum cytotoxic concentration (MCC)] were determined by microscopy (minimal changes in cell morphology).

3. 3. Molecular Modeling

3. 3. 1. Molecular Dynamics Simulations

Starting structure for reovirus type 1 (strain Lang) (T1L) protein was obtained from RCSB Protein Data Bank, which was obtained by X-ray diffraction with resolution of 2.2 Å (PDB ID: 4xc5).[11] It is a homotrimer structure. Three magnesium ions, which were coordinated to Asn375 and Thr454 residues of each monomer contributing to structural integrity were kept. Crystal water molecules were stripped. Sidechain atoms of some resiudes were missing so they were completed on YASARA Structure software.[38] Protonations states of each titratable residue were calculated on PROPKA server.[39] Upon this calculation the Asp362 residues of each monomer were protonated with pK_a values 12.83, 11.74, and 14.15, respectively. Other titratable residues were calculated to be in their default protonation states, acidic residues were deprotonated and basic residues were protonated.

This T1L protein model was subjected to 20 ns long classical molecular dynamics (MD) simulations, utilizing GROMACS 5.1.4 program[40–42] which was utilized with GROMOS force field GROMOS96 54A7.[43] Protein, with Mg^{2+} ions, was placed in truncated, cubic boxes with dimensions of 10.0 × 10.0 × 10.0 nm. These dimensions ensured that at any point of the simulation the proteins stayed in the simulation box. Single point charge (SPC) water molecules were placed into the box and total of 27 sodium

and chloride ions were added to neutralize the system.[44] Firstly, starting system was subsequently energy-minimized using the steepest descent method for 50,000 steps. Then, energy-minimized structures were taken for the production phase. MD simulation without any constraints was carried out using a constant number of particles (*N*), pressure (*P*), and temperature (*T*), *i.e.* NPT ensemble. The SETTLE algorithm was utilized to constrain the bond length and bond angle of the water molecules while the LINCS algorithm was used to constrain the bond length of the peptide.[45,46] Particle-mesh Ewald (PME) method was utilized to treat long-range electrostatic interactions.[47] A constant pressure of 1 bar was applied with a coupling constant of 1.0 ps and water molecules/ions were coupled separately to a bath at 303 K with a coupling constant of 0.1 ps. The equation of motion was integrated at 2 fs time steps using a leap-frog algorithm.[48] The tools available in the GROMACS and VMD 1.9.1. software were utilized to analyze trajectories.[49] The most representative structure of 20 ns simulation was obtained by clustering tool of GROMACS (g_cluster).

Docking poses, ligand bound structures, with the highest binding affinities, for ligands **6c** and **6f**, were subjected to further 20 ns long classical MD simulations to test the stability of ligands in these binding pockets, utilizing YASARA Structure software, which utilized YASARA2 force field.[50,51] Exactly the same conditions described above for T1L protein MD simulation, including box sizes, were applied. Binding free energies were calculated with the same software, md_analyzebindenergy macro.[38] This module calculates energies without the entropy term.

$$G = E_{bind} + E_{el} + E_{vdW} + G_{polar} + G_{nonpolar}$$

Here, the first three terms represent binding, electrostatic, and van der Waals interactions, respectively. G_{polar} and $G_{nonpolar}$ are polar and nonpolar contributions of solvation free energies, respectively. It is very similar to MM/PBSA for the entropy term, which can be neglected in the context of main goal of these calculations. Then, binding free energy is calculated by the following equation.

$$\text{Binding Energy} = (G_{Receptor} + G_{Ligand}) + (Gsolv_{Receptor} + Gsolv_{Ligand}) - (G_{Complex} + Gsolv_{Complex})$$

The first two terms stand for potential energies of the receptor and ligand, and the next two terms represent solvation energies of the receptor and ligand, and the last terms are potential and solvation energies of the complex.

3. 3. 2. Molecular Docking Simulations

All docking simulations were performed utilizing AutoDock Vina 1.1.2 software.[52] Protein structures were put into a 7.6 × 7.2 × 7.2 nm grid box to occupy the whole ligand-protein systems and the spacing was kept at 1.00 Å, a standard value for AutoDock Vina. Each docking trial produced 20 poses with the exhaustiveness value of 20.

Structures of ligands were optimized by using YASARA software with YAMBER force field.[50,51] Binding poses were grouped according to their binding affinity, high population of hits, and RMSD values. One binding pocket for each ligand, which produced the highest binding affinity, was assessed. AutoDock Vina uses a stochastic optimization algorithm thus, for each ligand docking simulations were repeated twice. Repetition of simulations produced similar binding results with highly similar binding affinities. Ligands in their most probable binding pockets were subjected to 20 ns long classical MD simulations, as described above.

4. Conclusions

These results demonstrate the importance of position 1 of the unsubstituted indole ring for selective activity against reovirus-1 as well as trifluoromethoxy and bromine substitution at position 5 of the indole ring. In compounds substituted with trifluoromethoxy and bromine at position 5 of the indole ring, 1-methyl substitution at position 1 of the indole ring caused a decrease in anti-reovirus-1 activity as well as an increase in cytoxicity. With molecular modeling analyses, the mechanisms of action of selective and non-toxic compounds were determined against reovirus-1.

Supplementary Material

The data that support the findings of this study are available in the Supplementary Material file.

Acknowledgements

This work was supported by The Scientific Research Projects Coordination Unit of Istanbul University (grant number TSG-2018-27798). Also, we want to thank for collaboration to Prof. Lieve Naesens from Department of Microbiology, Immunology and Transplantation, Rega Institute, Leuven, Belgium.

Declarations

Conflict of interest on behalf of all authors, the corresponding author states that there is no conflict of interest.

5. References

1. M. T. Heise, *Reference Module in Biomedical Sciences.* **2014**, B978-0-12-801238-3.00079-9. **DOI:**10.1016/B978-0-12-801238-3.00079-9
2. S. Payne: Viruses from understanding to investigation, USA,

Elsevier, Academic Press E-Publishing, **2017.**
DOI:10.1016/B978-0-12-803109-4.00009-X
3. J. D. Doyle, J. E. Stencel-Baerenwald, C. A. Copeland, J. P. Rhoads, J. J. Brown, K. L. Boyd, J. B. Atkinson, T. S. Dermody, *PLOS Pathog.* **2015**, *11(3)*, e1004693. **DOI:**10.1371/journal.ppat.1004693
4. A. H. Sharpe, B. N. Fields, in: W. K. Joklik (Ed.): Pathogenesis of Reovirus Infection, The Reoviridae, MA: E-Publishing Springer, Boston, **1983**, 229–285. **DOI:**10.1007/978-1-4899-0580-2
5. X. Zhang, H. Wu, C. Liu, J. Tian, L. Qu, *Infect. Genet. Evol.* **2015**, *34*, 415–422. **DOI:**10.1016/j.meegid.2015.06.008
6. T. Hotani, M. Tachibana, H. Mizuguchi, F. Sakurai, *Biochem. Biophys. Res. Commun.* **2015**, *460(4)*, 1041–1046. **DOI:**10.1016/j.bbrc.2015.03.147
7. P. Danthi, G. H. Holm, T. Stehle, T. S. Dermody, *Adv. Exp. Med. Biol.* **2013**, *790*, 42–71. https://dx.doi.org/10.1007%2F978-1-4614-7651-1_3
8. K. W. Boehme, M. Ikizler, T. Kobayashi, T. S. Dermody, *Methods.* **2011**, *55(2)*, 109–113. **DOI:**10.1016/j.ymeth.2011.07.002
9. D. H. Rubin, M. J. Kornstein, A. O. Anderson, *J. Virol.* **1985**, *53(2)*, 391–398. **DOI:**10.1128/jvi.53.2.391-398.1985
10. A. Kapikian, R. E. Shope, in: S. Baron (Ed.): Chapter 63. Rotaviruses, Reoviruses, Coltiviruses and Orbiviruses, Medical Microbiology, TX: University of Texas Medical Branch at Galveston, Galveston, **1996**.
11. E. Stettner, M. H. Dietrich, K. Reiss, T. S. Dermody, T. Stehle, *J. Virol.* **2015**, *89(11)*, 6136–6140. **DOI:**10.1128/JVI.00433-15
12. J. C. Forrest, T. S. Dermody, *J. Virol.* **2003**, *77(17)*, 9109–9115. **DOI:**10.1128/JVI.77.17.9109-9115.2003
13. T. R. Bal, B. Anand, P. Yogeeswari, D. Sririam, *Bioorg. Med. Chem. Lett.* **2005**, *15(20)*, 4451–4455. **DOI:**10.1016/j.bmcl.2005.07.046
14. N. Terzioğlu, N. Karalı, A. Gürsoy, C. Pannecouque, P. Leysen, J. Pashuyse, J. Neyts, E. De Clercq, *ARKIVOC* **2006**, *(i)*, 109–118. **DOI:**10.3998/ark.5550190.0007.113
15. D. Banerjee, P. Yogeeswari, P. Bhat, A. Thomas, M. Srividya, D. Sriram, *Eur. J. Med. Chem.* **2011**, *46(1)*, 106–121. **DOI:**10.1016/j.ejmech.2010.10.020
16. S. Y. Abbas, A. A. Farag, Y. A. Ammar, A. A. Atrees, A. F. Mohamed, A. A. El-Henawy, *Monatsh. Chem.* **2013**, *144*, 1725–1733. **DOI:**10.1007/s00706-013-1034-3
17. Z. Ş. Sevinçli, G. N. Duran, M. Özbil, N. Karalı, *Bioorg. Chem.* **2020**, *104*, 104202. **DOI:**10.1016/j.bioorg.2020.104202
18. D. J. Bauer, P. W. Sadler, *Brit. J. Pharmacol.* **1960**, *15(1)*, 101–110. **DOI:**10.1111/j.1476-5381.1960.tb01216.x
19. P. W. Sadler, *Annals of the New York Academy of Sciences.* **1965**, *130(1)*, 71–79. **DOI:**10.1111/j.1749-6632.1965.tb12541.x
20. L. Sherman, F. Edelstein, G. Shtacher, M. Avramoff, Y. Teitz, *J. Gen. Virol.* **1980**, *46(1)*, 195–203. **DOI:**10.1099/0022-1317-46-1-195
21. Y. Teitz, D. Ronen, A. Vansover, T. Stematsky, J. L. Riggs, *Antiviral Res.* **1994**, *24(4)*, 305–314. **DOI:**10.1016/0166-3542(94)90077-9
22. I-J. Kang, L-W. Wang, T-A. Hsu, A. Yueh, C-C. Lee, Y-C. Lee, C-Y. Lee, Y-S. Chao, S-R. Shih, J-H. Chern, *Bioorg. Med. Chem. Lett.* **2011**, *21(7)*, 1948–1952. **DOI:**10.1016/j.bmcl.2011.02.037
23. M. C. Pirrung, S. V. Pansare, K. Das Sarma, K. A. Keith, E. R. Kern, *J. Med. Chem.* **2005**, *48(8)*, 3045–3050. **DOI:**10.1021/jm049147h
24. P. Selvam, N. Murugesh, M. Chandramohan, K. A. Keith, E. R. Kern, *Antivir. Chem. Chemother.* **2006**, *17(2)*, 107–110. **DOI:**10.1177/095632020601700206
25. P. Selvam, N. Murugesh, M. Chandramohan, R. W. Sidwell, M. K. Wandersee, D. F. Smee, *Antivir. Chem. Chemother.* **2006**, *17(5)*, 269–274. **DOI:**10.1177/095632020601700504
26. P. Selvam, M. Chandramohan, B. L. Hurst, D. F. Smee, *Antivir. Chem. Chemother.* **2010**, *20(3)*, 143–146. **DOI:**10.3851/IMP1471
27. P. Selvam, N. Murugesh, M. Chandramohan, E. De Clercq, E. Keyaerts, L. Vijgen, P. Maes, J. Neyts, M. V. Ranst, *Indian J. Pharm. Sci.* **2008**, *70(1)*, 91–94. **DOI:**10.4103/0250-474X.40339
28. N. Karalı, A. Akdemir, F. Göktaş, P. Eraslan-Elma, A. Angeli, M. Kızılırmak, C. T. Supuran, *Bioorg. Med. Chem.* **2017**, *25(14)*, 3714–3718. **DOI:**10.1016/j.bmc.2017.05.029
29. K. Reiss, J. E. Stencel, Y. Liu, B. S. Blaum, D. M. Reiter, T. Feizi, T. S. Dermody, T. Stehle, *PLOS Pathog.* **2012**, *8(12)*, e1003078. **DOI:**10.1371/journal.ppat.1003078
30. S. J. Garden, J. C. Torres, L. E. DaSilva, A. C. Pinto, *Synth. Commun.* **1998**, *28(9)*, 1679–1689. **DOI:**10.1080/00397919808006872
31. K. L. Vine, J. M. Locke, M. Ranson, S. G. Pyne, J. B. Bremner, *J. Med. Chem.* **2007**, *50(21)*, 5109–5117. **DOI:**10.1021/jm0704189
32. N. Karalı, P. Eraslan-Elma, G. Cihan Üstündağ, F. Göktaş, New 1-substituted 1*H*-indole-2,3-dione compounds ve synthesis methods, *Turk. Pat. Appl.* Patent Number TR 2015 015912 B, date of patent December 11, **2015**.
33. R. L. McKee, R. W. Bost, *J. Am. Chem. Soc.* **1946**, *68(12)*, 2506–2507. **DOI:**10.1021/ja01216a022
34. N. Karalı, P. Eraslan-Elma, F. Göktaş, Process for preparation of N-[(aminosulfonyl)phenyl]-2-(1,2-dihydro-2-oxo-3H-indol-3-ylidene)hydrazinecarbothioamide derivatives, *Turk. Pat. Appl.* Patent Number TR 2015 016135 B, date of patent December 15, **2015**.
35. N. Karalı, F. Göktaş, G. Cihan-Üstündağ, P. Eraslan, N-[(-Aminosulfonyl)phenyl]-2-(1,2-dihydro-2-oxo-3*H*-indol-3-ylidene)hydrazinecarbothioamide derivatives for treating cancer and immunological disorders, *PCT Int. Appl.* Patent Number WO 2017099695 A1, date of patent June 15, **2017**.
36. L. Naesens, E. Vanderlinden, E. Roth, J. Jeko, G. Andrei, R. Snoeck, C. Pannecouque, E. Illyés, G. Batta, P. Herczegh, F. Sztaricskai, *Antiviral Res.* **2009**, *82(1)*, 89–94. **DOI:**10.1016/j.antiviral.2009.01.003
37. C. Pannecouque, D. Daelemans, E. De Clercq, *Nat. Protoc.* **2008**, *3*, 427–434. **DOI:**10.1038/nprot.2007.517
38. E. Krieger, G. Koraimann, G. Vriend, *Proteins.* **2002**, *47(3)*,

393–402. **DOI:**10.1002/prot.10104
39. T. J. Dolinsky, J. E. Nielsen, J. A. McCammon, N. A. Baker, *Nucleic Acids Res.* **2004**, *32 (Web Server issue)*, W665-W667. **DOI:**10.1093/nar/gkh381
40. H. J. C. Berendsen, D. Van der Spoel, D. E. Van Drunen, *Computer Physics Communications.* **1995**, *91(1–3)*, 43–56. **DOI:**10.1016/0010-4655(95)00042-E
41. E. Lindahl, B. Hess, D. Van der Spoel, *J. Mol. Model.* **2001**, *7*, 306–317. **DOI:**10.1007/s008940100045
42. D. Van Der Spoel, E. Lindahl, B. Hess, G. Groenhof, A. E. Mark, H. J. C. Berendsen, *J. Comput. Chem.* **2005**, *26(16)*, 1701–1718. **DOI:**10.1002/jcc.20291
43. N. Schmid, A. P. Eichenberger, A. Choutko, S. Riniker, M. Winger, A. E. Mark, W. F. Van Gunsteren, *Eur. Biophys. J.* **2011**, *40*, 843. **DOI:**10.1007/s00249-011-0700-9
44. P. E. Smith, W. F. Van Gunsteren, *Chemical Physics Letters.* **1993**, *215(4)*, 315–318. **DOI:**10.1016/0009-2614(93)85720-9
45. S. Miyamoto, P. A. Kollman, *J. Comput. Chem.* **1992**, *13(8)*, 952–962. **DOI:**10.1002/jcc.540130805
46. B. Hess, H. Bekker, H. J. C. Berendsen, J. G. E. M. Fraaije, *J. Comput. Chem.* **1997**, *18(12)*, 1463–1472. **DOI:**10.1002/(SICI)1096-987X(199709)18:12<1463::AID-JCC4>3.0.CO;2-H
47. T. A. Darden, D. York, L. Pedersen, *J. Chem. Phys.* **1993**, *98(12)*, 10089–10092. **DOI:**10.1063/1.464397
48. R. W. Hockney, S. P. Goel, J. W. Eastwood, *J. Comput. Phys.* **1974**, *14(2)*, 148–158. **DOI:**10.1016/0021-9991(74)90010-2
49. W. Humphrey, A. Dalke, K. Schulten, *J. Mol. Graph.* **1996**, *14(1)*, 33–38. **DOI:**10.1016/0263-7855(96)00018-5
50. E. Krieger, G. Vriend, *Bioinformatics.* **2002**, *18(2)*, 315–318. **DOI:**10.1093/bioinformatics/18.2.315
51. E. Krieger, T. Darden, S. B. Nabuurs, A. Finkelstein, G. Vriend, *Proteins.* **2004**, *57(4)*, 678–683. **DOI:**10.1002/prot.20251
52. O. Trott, A. J. Olson, *J. Comput. Chem.* **2010**, *31(2)*, 455–461. **DOI:**10.1002/jcc.21334

Povzetek

Preučili smo aktivnost 1*H*-indol-2,3-dion 3-[4-(4-sulfamoilfenil)tiosemikarbazonov] **6a–j** proti naslednjim virusom: para-influenca-3, reovirus-1, sindbis, coxsackie B4 in Punto Toro. Sintetizirali smo nove 1-metil-1*H*-indol-2,3-dion 3-[4-(4-sulfamoilfenil)tiosemikarbazone] **7a–c** in določili vpliv metilnega substituenta na položaju 1 indolnega sistema na antivirusno aktivnost. Rezultati kažejo, da sta 5-trifluorometoksi substituirana spojina **6c** (EC_{50} 2–9 μM) in 5-bromo substituirana **6f** (EC_{50} 2–3 μM) nestrupeni ter da kažeta selektivno antivirusno aktivnost; po drugi strani pa niti vsi standardi niso aktivni proti reovirusu-1. Študije molekulskega sidranja spojin **6c** and **6f** smo izvedli z namenom določanja mesta vezave v reovirusu-1. Trifluorometoksi and bromino substituenta na položaju 5 indolnega sistema zagotavljata selektivno antivirusno aktivnost; metilni substituent na položaju 1 indolnega sistema pa občutno zmanjša aktivnost proti reovirusu-1, hkrati pa ima povečano strupenost.